Fall 2010

Standoff Raman spectroscopy detection of trace explosives

Abhijeet Singh

Department:

STANDOFF RAMAN SPECTROSCOPY DETECTION OF TRACE EXPLOSIVES

by

ABHIJEET SINGH

A THESIS

Presented to the Faculty of the Graduate School of the

MISSOURI UNIVERSITY OF SCIENCE AND TECHNOLOGY

In Partial Fulfillment of the Requirements for the Degree

MASTER OF SCIENCE IN ELECTRICAL ENGINEERING

2010

Approved by

Dr. Sanjeev Agarwal, Advisor

Dr. Sahra Sedigh Sarvestani

Dr. Randy Moss

ABSTRACT

During the 2003-present Iraq war, Improvised Explosive Devices (IEDs) are being used extensively by the terrorists against the coalition forces and these IEDs were responsible for 40% of coalition force casualties, by the end of 2007. As these IEDs are not based on standard production formulae, their tracking and detection becomes extremely complicated. Laser Induced Breakdown Spectroscopy (LIBS) and Raman Spectroscopy are among the many techniques that have shown promise in detection of explosive compounds. However, the performance of these systems is dependent on the concentration of explosives and ambient noise.

The research presented in this thesis applies signal processing techniques to Raman spectra of a sample to detect the presence of explosives in trace quantities, at a standoff distance. Partial least squares-Discriminant analysis (PLS-DA) was used to identify peaks in the Raman spectra of the sample, which could better differentiate explosive and non-explosive samples. Since peak strengths are vulnerable to noise, our algorithm uses peak energies instead, by fitting Lorentzian or Gaussian curves about the peak locations. An automatic peak detection and fitting algorithm was developed for this purpose. Also, a wavelet based signal denoising algorithm was implemented to remove noise from the Raman Spectra. Further, a multi-sensor fusion algorithm was developed to combine the results from Laser Induced Breakdown Spectroscopy (LIBS) and Raman Spectroscopy to generate more accurate detection results.

The multi-sensor fusion algorithm gave more accurate detection results, a higher probability of detection and lower probability of false alarms, as compared to the results obtained from individual spectroscopic techniques, i.e. Raman Spectroscopy and Laser Induced Breakdown Spectroscopy alone.

ACKNOWLEDGMENTS

First and foremost, I would like to thank my parents and grandmother for motivating me to pursue the master's degree. I would like to thank Dr. Sanjeev Agarwal for giving me an opportunity to work on this project. Without his tireless efforts and endless solutions this project would not have completed. Special thanks to Dr. Sahra Sedigh and Dr. Randy Moss for serving on my thesis committee. I am grateful to Pratik Shah for being a great team member and for helping me and guiding me throughout the project. A special thanks to all ARIA lab students, especially Dheeraj Singiresu who has always been there whenever I needed help.

TABLE OF CONTENTS

Page

LIST OF ILLUSTRATIONS

LIST OF TABLES

1 INTRODUCTION

The advent of the 21st century saw rapid technological advancements, both in hardware and software. Research and development was at its peak, with countries striving hard to utilize state of the art technology to fight the war against terrorism. On the other hand, terrorists were using similar technology to develop deadlier weapons and explosives. Improvised Explosive Devices (IEDs) became the weapon-of-choice of terrorists around the world and were frequently used against national armies during war and against civilians to spread terror. The popularity of IEDs among terrorists can be based on the fact that IEDs can be prepared almost anywhere with materials acquired from agricultural and medical supplies and do not require high technical knowledge. Also, the detection of IEDs becomes extremely complicated since they are not based on standard production formulae. Currently available detection techniques provide satisfactory results for bulk quantities of explosive but fail when the quantity of explosives is in trace amounts, i.e. in the order of micrograms. IED precursors are trace amount of explosives left behind usually while handling or transporting IEDs. Detection of such IED precursors becomes increasingly difficult through currently available techniques because of the concentration of explosives available for analysis and the environment in which they are present. Contaminants such as dust, oil, moisture, etc. hinder the explosive detection process further by affecting the SNR of the spectrum obtained for analysis.

The research presented in thesis is based on a standoff explosive detection technique using Raman spectroscopy to collect spectral data for analysis. "*Standoff explosive detection involves passive and active methods for sensing the presence of explosive devices when vital assets and those individuals monitoring, operating, and responding to the means of detection are physically separated from the explosive device. The physical separation should put the individuals and vital assets outside the zone of severe damage from a potential detonation of the device"* [1]. Using Raman spectroscopy, samples can be investigated from a safe distance without putting individuals and vital assets in the damage zone. The spectral data collected using Raman

spectroscopy provides information on molecular structure and chemical composition of the sample. For this research work, the standoff distance is in the range of 20 [m] and the concentration of explosive is on the order of micro-grams. Raman spectroscopy has the following advantages:

- Specificity: Raman Spectroscopy exhibits high specificity. Several varying resonance Raman spectra of the same molecule can be collected by varying the wavelength of the laser used for sample excitation. The Raman spectra of a particular part of the molecule will be enhanced if the excitation wavelength matches the absorption of that specific part of the molecule.

- Aqueous system analysis: The IR spectrum of water is strong and complex. IR spectroscopy of water based samples becomes impossible since the water bands produces heavy interference and overlaps with the spectrum of the sample. The Raman spectrum of water is weak and so it allows good spectrum of the water-based samples to be collected.

- Non-destructive: Raman spectroscopy does not require sample preparation unlike other spectroscopic techniques. Raman involves only illuminating the sample from a distance using a laser and collecting the scattered photons.

- Real-Time: Raman spectroscopy can be used in real time applications because the Raman spectrum can be acquires in a matter of seconds.

A literature review about existing and potential standoff explosive detection techniques is done in Sec 2. Several explosives in varying concentrations were analyzed as a part of this research. The complete set of data used for analysis and the hardware used for Raman spectral data collection is described in Sec 3. The spectral data collected has many outliers which needed to be removed before further analysis. As a part of preprocessing of data, a signal denoising algorithm was implemented which removes noise from the Raman spectra using a wavelet transformation and Partial Least Squares-Discriminant Analysis (PLS-DA) was used to find peaks which would better discriminate explosive and non explosive samples. Section 4 provides details about all the techniques used for preprocessing the spectral data. Automatic curve fitting is an extension to the

local curve fitting described by Shah in [3] and is one of the signal processing techniques described in this thesis work. Multi-sensor fusion was used to combine decision values obtained from Laser Induce Breakdown Spectroscopy (LIBS) and Raman in an attempt to increase the Probability of Detection (PD) and reduce the Probability of False Alarm (PFA). Signal processing techniques are described in Sec 5. A detailed discussion of the results is provided in Sec 6. Figure 1.1 below summarizes the IED precursor detection process proposed in this thesis work. LIBS operations were developed and performed as a part of the research work done by Shah [3], and the LIBS decision value was directly used for the Multi-Sensor Fusion algorithm.

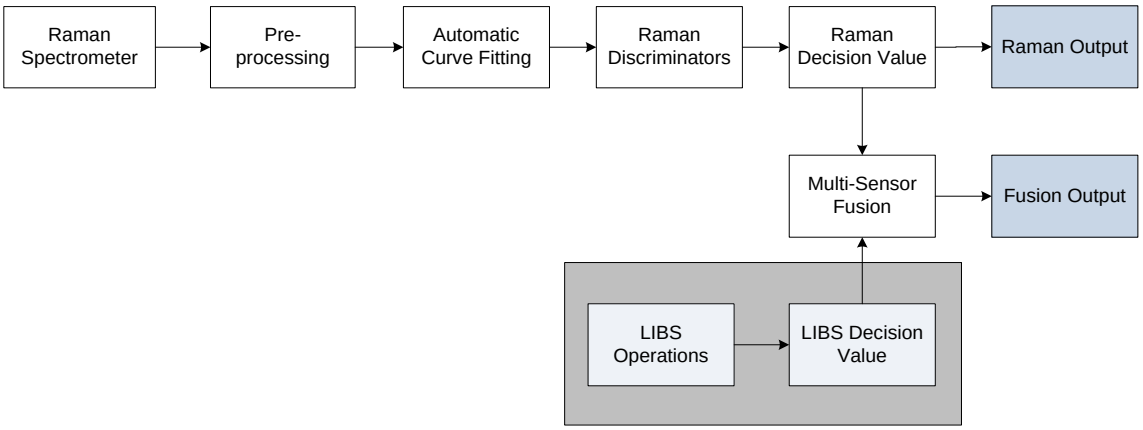

Figure 1.1. The proposed IED detection process

2 BACKGROUND AND RELATED WORK

Several explosive detection techniques exist based on a wide variety of current and developing technologies. Explosive detection solutions can be broadly classified into bulk detection techniques and trace detection techniques. Bulk detection techniques utilize the form factor of the explosives by imaging characteristic shapes of the components of the explosive like detonators, wires etc. or by analyzing the chemical properties of the explosive composition. One of the pre-requisite to bulk detection techniques is high concentration of explosives. In the case of trace amount of explosives, the performance of bulk detection techniques degrades considerably. Trace detection techniques are primarily focused on providing IED detection solutions for explosives present in trace amounts. Trace explosive detection techniques are based off the vapors emitted by the explosive or residue of explosives which are deposited on surfaces during handling. Section 2.1 and Section 2.2 below explain in detail the techniques for bulk and trace detection of explosives.

For standoff explosive detection techniques, the operating distance depends on the size of the explosive and the amount of standoff distance is 10 [m] or more [1]. An ideal explosive detection technique would classify all explosive samples as explosives and would not misclassify any non-explosive sample as explosive, i.e. the explosive detection technique would show 100 % probability of detection (PD) and 0% probability of false alarms (PFA). Due to environmental variations, ambient noise, etc. such ideal explosive detection techniques do not exist and systems with a high probability of detection and a low probability of false alarms are considered satisfactory for explosive detection. Explosive detection is usually a very complex process with the technique varying depending upon the scenario of the explosive state. Each explosive detection technique has to compensate for several limitations, some of which are caused by fundamental physics while some are the result of the scenario of the particular explosive.

2.1 BULK EXPLOSIVE DETECTION

Imaging techniques integrated with computer tomography have been successfully used to estimate the densities of objects, which forms the basis of Bulk explosive detection techniques. Typical high explosives like PETN and RDX have total densities between 1.2 and 1.8 g/cm^3 [1]. Moreover, the form factor of bulk explosives can be captured by means of imaging techniques like X-Rays, infrared imaging, etc. and be used for detection. Bulk explosives have characteristic spatial features and are composed of unique components like metal parts, batteries and wires. These features are often good indicators of the presence of bulk explosives. The optical properties of explosives – reflection, absorption and scattering, are used to create a database for different spectral bands using different imaging techniques. This database is then used for image analysis for several bulk explosive detection techniques. Sections below give a brief description of promising bulk detection techniques.

X-Rays have been widely used for detection of explosives and other smuggled objects like drugs, illegal weapons, etc. The two modes in which X-Ray imaging can be used for detection are transmission and backscatter. In the transmission mode, a detector is required on the opposite side of the transmitter to capture images. An inexpensive wireless camera is used to monitor the detector. An image is captured on the detector because of the absorption of the X-Rays by denser objects like explosives and concealed weapons. In the backscatter X-Ray imaging mode, both the transmitter and detector are located on the same side of the object being imaged. The backscattered X-Ray imaging mode generates images in which objects can be differentiated based on their density. For heavier elements like metals, the atoms contain more electrons as compared to lighter elements. The incident and backscattered X-Rays penetrate deep inside the material and generate images based on the electron density of atoms. Thus, heavier element materials can be differentiated from lighter element materials in backscattered X-Ray images. Yang et al. [6] have successfully combined dual energy X-Ray imaging and photoneutron induced γ-ray analysis to improve the capability of contraband detection. X-Ray imaging techniques can identify different materials based on atomic number like organic, inorganic, heavy metal, etc. and γ-ray analysis is then performed on the organic material

area. Although the X-Ray imaging technique has shown promise in the field of standoff explosive detection, the harmful ionization effects of X-Rays are unavoidable and remain one of the major shortcomings of the X-ray imaging technique.

Electromagnetic imaging techniques like Infrared (IR) imaging and terahertz imaging, have shown promise for bulk detection of explosives. IR imaging can be used to detect thermal radiation of objects using simple low-cost IR cameras. Such thermal imaging techniques prove to be useful for detecting suicide bombers, where the explosive is often covered by clothing. The IR imaging techniques have been successful at detection of explosives at standoff distances but lack the specificity required for discriminating explosive types. IR imaging techniques are often used in conjunction with other detection techniques, where the IR imaging technique is used to perform preliminary detection of potential explosive carriers. Along with bulk explosive detection, infrared photo-thermal imaging has shown promise for trace explosive detection [7]. Furstenberg et al. have used miniature quantum cascade lasers (QCLs) to illuminate trace explosive sample and captured the thermal signal using an infrared camera. The selectivity and sensitivity of this technique can be increased by varying the incident wavelength of the laser to match the strong absorption bands in the explosive traces. Another electromagnetic imaging technique which has shown promise in detection of trace amount of explosives at standoff distances is Terahertz (THz) Time-Domain Spectroscopy [8]. Kong and Wu have successfully demonstrated a Terahertz Time-Domain Spectroscopy (THz-TDS) technique for detection of low-density explosives as well as bulk explosives. The THz pulses which are reflected or transmitted through the sample are collected and the change in electric field of the pulses is measured using THz-TDS technique. For radiation frequency in the Terahertz range i.e. wavelengths between 100 micrometer and 1 millimeter, several materials like clothing, paper, plastic etc become nearly transparent. At such high frequencies, the radiation can easily penetrate several dielectric materials. Moreover, THz waves have very low photon energies as compared to X-Ray photons, so they do not cause harmful ionization effects like X-Ray and nuclear detection methods. Techniques involving THz radiation usually suffer from low sensitivity because of the low absorption peaks in the THz band. Also, absorption of THz radiation by water vapor in the air is another major issue with detection techniques

involving THz spectrum band. Other techniques for bulk detection of explosives have been proposed like neutron and γ-ray, magnetic resonance techniques, etc. Harmful ionization effects, insufficient sensitivity and/or specificity and degradation of performance at standoff distances are the main reasons which have hindered the progress for these techniques for standoff bulk explosive detection.

2.2 TRACE EXPLOSIVE DETECTION

Detection of explosives in trace amounts and at standoff distances becomes extremely challenging because of the low concentration of explosives available for analysis and the presence of environmental contaminants like dust, oil, etc. which further hamper the detection process. Griffy[9] has shown that sampling surfaces for explosive residue is more efficient than probing the air around the explosive for vapors. Several techniques have been proposed and have been extensively researched for trace explosive detection, which essentially involves inspecting the surface for explosive residues and performing further analysis for accurate explosive detection. Electronic and chemical techniques like mass spectroscopy, surface acoustic wave, electron capture detector, etc. have shown promise for trace explosive detection but suffer from low sensitivity and low selectivity. Techniques involving biosensors like dogs, bees, etc. have been successful in trace detection but human intervention prevents these techniques to be applied at standoff distances. Optical absorption techniques use their UV electronic and infrared vibrational resonances to identify explosive molecules. Such techniques usually require expensive and fragile apparatus to capture and analyze large samples in order to increase the signal-to-noise ratio to the desired level. Techniques involving optical fluorescence have been used for standoff explosive detection. A laser is used to induce fluorescence in the explosive particles in the UV where they strongly absorb and decompose into fragments which exhibit fluorescence properties. These patterns can then be captured at standoff distance and used for detection. The lack of very high sensitivity and problems of removing the fluorescence with environmental contaminants are the major disadvantages of this technique.

Linear optical techniques like laser, light detection and ranging (LIDAR), differential absorption LIDAR (DIAL) and differential reflectance LIDAR (DIRL) have been successful in trace detection of explosives. The basic principle involved in LIDAR is that the explosive molecules absorb when the source light is tuned to a molecular resonance which is typically a vibrational resonance in the IR spectral range. Thus, the radiation from the illuminating source is backscattered to a detector with the explosive molecules absorbing some radiation. This absorption tends to attenuate the radiation indicating presence of an explosive. Because of backscattering resulting from particulates in the air at standoff distances, the sensitivity of such systems are limited and are usually used for sensing rather than imaging. Other spectroscopic techniques like Laser Induced Breakdown Spectroscopy (LIBS) and Raman Spectroscopy have shown promise in detection of explosive residues at standoff distances. In LIBS process, the plasma created by laser-induced breakdown is analyzed for spectral emission from ionic, atomic and molecular species [11]. The LIBS spectra are analyzed and the presence of an individual element in the sample is based on the existence of an emission line in the spectra. The strength of the emission line determines the relative abundance of the individual element in the compound. The compound (sample) interrogated can be identified based on the presence of individual elements and the relative abundance of those elements in the plasma. Such explosive identification process is complicated by the fact that some compounds have similar elemental content and may produce similar signature spectra. Gottfried et al. [12] have shown that LIBS can be successfully used for detection of trace amount of explosive samples at standoff distances of 50 m. They have used LIBS along with chemometric techniques like Principal Component Analysis (PCA) and Partial Least Square – Discriminant Analysis (PLS-DA) for detection of explosive samples. Alexander et al. [13] have used LIBS for detection of heavy metals like As, Cd, Cr, Hg, Pb and Zn in soil and water. They have used a Nd:YAG laser operating at 50-100 mJ at $\lambda = 1.06$ μm for generating the plasma on the surface of the sample and recorded the atomic emission lines using an optical multichannel analyzer (OMA). They suggest the use of Si emission lines as a reference for heavy metal emission lines to generate intensity ratios. The dependence of LIBS on experimental conditions like variation of laser pulse energy or alignment of spectra collection system can be reduced used intensity ratio for detection.

Another approach for molecular analysis of compounds at standoff distanced is Raman spectroscopy which uses a laser to excite different vibrational modes of a molecule. The laser beam when impinged upon the sample causes the photons to be absorbed by the material and scattered. The incident photon causes an electron to jump to a virtual higher energy state and then the electron decays to a lower energy level emitting a scattered photon with corresponding wavelength dependent upon the final state of the electron. Majority of the scattered photons have the same wavelength as the incident photons (Rayleigh scattering) but few photons, approximately 1 in 10^7, are shifted to a different wavelength (Raman scattering). If the Raman scattered photons are shifted to longer wavelengths they are called Stokes shift, whereas the Raman scattered photons shifted to shorter wavelengths are called Anti-stokes shift. Usually, Stoke shift photons are more dominant than Anti-stoke shift photons and are frequently used in spectroscopy. These energy transitions arise from molecular vibrations and can be used to identify the molecule. The energy of the transitions is plotted as emission spectrum and analyzed to find the presence of explosive compounds. A typical Raman spectrum is a plot of the intensity of Raman scattered radiation as a function of its frequency difference from the incident radiation (usually in units of wavenumbers, cm^{-1}). In the Raman spectra, the dominant Rayleigh scattered photons tend to overlap the relatively weaker Stoke shift photons. Gaft and Nagli [14] have proposed the use of UV-gated Raman techniques to counter the effect of Rayleigh scattering masking the weak Raman signal. UV excited Raman signals tend to be 100-200 times stronger compared to Raman signal generated by green laser (532 nm) and can be used to obtain strong Raman signals of trace explosive samples at standoff distances. They successfully applied gated Raman spectroscopic techniques for detection of explosive residuals at standoff distances up to 30 m. It can be inferred that several industrial and homemade explosives have very specific Raman fingerprints which makes Raman spectroscopy one of the more suitable technique for standoff trace explosive detection.

Although both LIBS and Raman spectroscopy have been successful in detection of trace explosives at standoff distances, individually they suffer from some inherent disadvantages which limit the performance of the individual sensing system. The

orthogonal nature of LIBS and Raman spectroscopy and the complementary information provided by each spectroscopic technique makes them ideal candidates for sensor fusion process. The Raman system is characteristic of highly specific molecular analysis whereas LIBS is characteristic of highly sensitive elemental analysis. The combination of LIBS and Raman spectroscopy causes a trade-off between the high sensitivity of LIBS and high specificity of Raman to increase the overall Probability of Detection and decrease Probability of False Alarms of the system. Wentworth et al. [14] have successfully demonstrated detection of trace explosive at moderate standoff distances using Raman hyperspectral imaging. They have developed a concept of combining LIBS and Raman standoff optical sensor into a single system for detection of hazardous materials. Miziolek et al. have applied LIBS and Raman fusion technique to CBE materials and have demonstrated the effectiveness of a combined system over individual spectroscopic techniques.

3 DESIGN OF EXPERIMENT

3.1 HARDWARE DESCRIPTION

The data used for study in this thesis work has been collected using the experimental setup described by Waterbury et al. [2]. Raman spectra of explosive and non-explosive samples have been recorded using a fully integrated UV Townsend Effect Plasma Spectroscopy (TEPS) -Raman system. TEPS Raman Explosive Detection System (TREDS-2) hardware, shown in Figure 3.1, which implements TEPS because of the 25-300 times increase in signal strength compared to single pulse LIBS. This tremendous signal enhancement provides sufficient design margin thereby allowing the laser wavelengths to be shifted to the UV for λ^{-4} Raman Enhancement and Eye Safety implications. The TREDS-2 system consists of a Q-switched 266 nm 4x Nd:YAG laser (Frequency Quadrupled Quantel Brilliant B) for Raman excitation and TEPS plasma ignition. The laser is focused onto the target using a custom designed beam expander and focusing optics. The plasma produced on the target was collected using a 14 in diameter telescope (Meade LX200-14) which was fiber coupled to an Andor Spectrometer (Shamrock SR303) and ICCD Camera (DH740-18F).

(a) Model of TREDS-2 TEPS/Raman system (b) TREDS-2 in a field test

Figure 3.1. The TREDS-2 system used for data collection

3.2 DATA

Analysis was performed on two sets of Raman data. The first dataset consisted of four types of explosive in this dataset with varying concentrations. There were no bare substrate samples in this dataset. The low concentration samples of all four explosives were combined to generate a common non-explosive dataset. All low concentration samples were included in the training dataset, during training for a particular explosive type. For e.g., during training for specimen A samples, the training dataset included low concentration samples of specimen A, B, C and D along with high concentration samples of specimen A. The distribution of explosive and non-explosive sample types is shown in Table 3.1.

Table 3.1. Distribution of data by sample type and concentration

Sample	Low Concentration (Non-explosive)	High Concentration (Explosive)
A	7	11
B	17	10
C	17	23
D	9	10
TOTAL	50	54

Spectra of each of the explosive types are shown below in Figure 3.2. The DC baseline and saturated peaks were removed from each spectrum before performing further analysis. Section 4 describes the data pre-processing methods in detail. The second dataset included the Raman data used for multi-spectral fusion analysis. This set of data had Specimen E samples and did not contain any non-explosive samples. Again,

the low concentration samples were treated as non-explosives and higher concentration samples were treated as explosives. The Raman fusion data is described in detail in Section 3.2 below. Due to the limited Raman data available for analysis, the training and testing was performed on the same dataset.

3.3 FUSION DATA

Decision level fusion was performed on LIBS and Raman spectra of specimen E. For a particular concentration of explosives, the LIBS and Raman spectra were collected from the same region and not from the same spot. Although it is advisable to collect samples from the same spot for fusion algorithms, samples from the same region produced satisfactory results and showed the effectiveness of our multi-sensor fusion algorithm. The fusion algorithm is described in Section 5.4 and the results of multi-sensor fusion are discussed in Section 6.2.

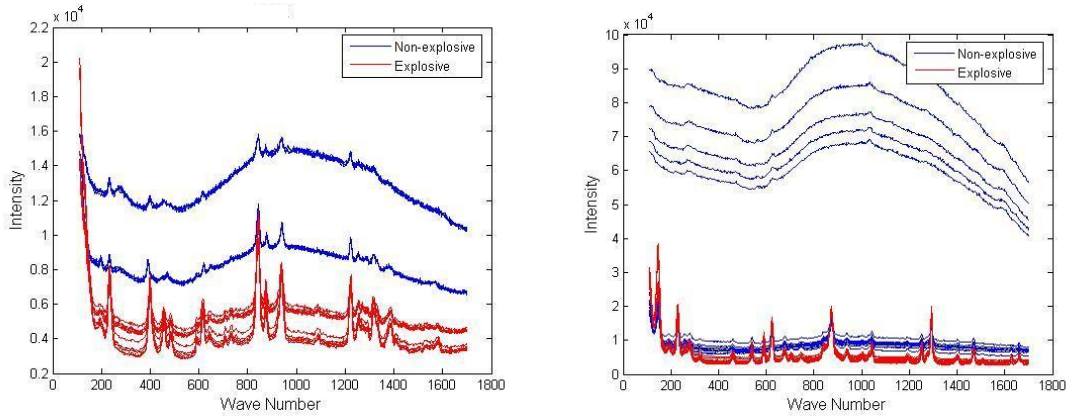

(a) Specimen B (b) Specimen C

Figure 3.2. Raman spectra for different sample type

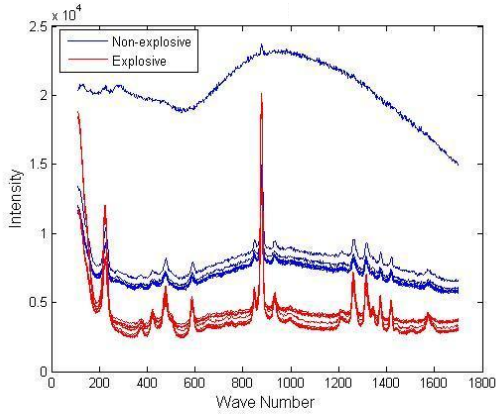

(c) Specimen A

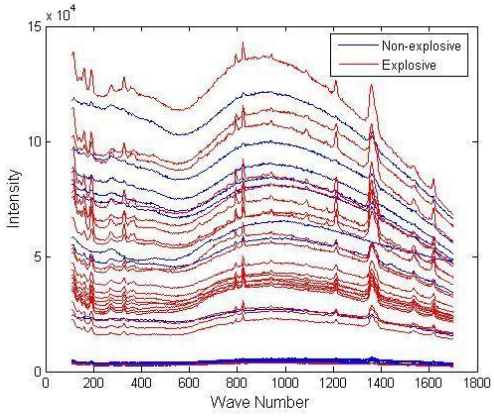

(d) Specimen D

Figure 3.2. Raman spectra for different sample type (cont.)

The specimen E fusion data samples were of varying concentrations. Since there were no samples from bare substrate, the samples with low concentration, were used as non-explosives whereas the samples with high concentration were used as explosives during analysis.

Table 3.2. Distribution of fusion data by sample type and spectroscopic technique

Data Type	**No. of Samples**
Raman Explosive	36
LIBS Explosive	17
Raman Non-explosive	32
LIBS Non-explosive	18

The purpose of this evaluation was to show the effect of fusion in better discrimination between explosives and non-explosives or in this case, high concentration and low concentration samples. Table 3.2 shows the distribution of the number of samples for LIBS and Raman. Figure 3.3 shows the Raman and LIBS spectra of explosive and non-explosive sample type used for multi-sensor fusion analysis.

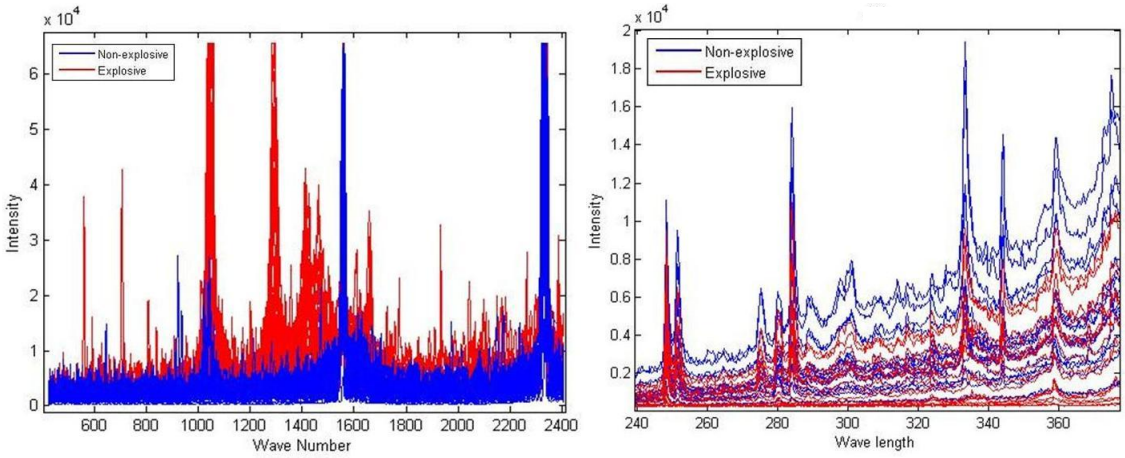

(a) Raman spectra (b) LIBS spectra

Figure 3.3. Fusion data for Raman and LIBS multi-sensor fusion

4 PRE-PROCESSING OF DATA

Raman spectral data was collected by using the experimental setup described in Sec 3. Data was collected on different days and different times and in varying environmental conditions. Several factors affect the spectral data collected like the concentration of samples, contaminants near samples, etc. The hardware used to collect data is also responsible for adding artifacts to the spectra. High intensity peaks can be cut-off due to limitations of the data collection equipment leading to saturated data. Variations in spectra like shifts in peak location, changes in peak intensities and widths are frequently observed. Also, CCD detectors inherit single shot noise which is characterized by variance proportional to the mean value of the measurement. Moreover, Raman spectra are plagued by high intensity spikes caused by cosmic ray events. Any high radiation event from local or extraterrestrial sources during data capture can lead to such cosmic spikes in the spectra. These cosmic spikes can overlap with discriminatory peaks in the spectra and vital information can be lost. It is essential to filter such artifacts and noise before performing further analysis.

4.1 REMOVAL OF BAD DATA

An outlier can be described as an observation which is present at an abnormal distance from other observations in the sample space. It is important to define what will be classified as an outlier and is largely dependent on the sample space available. We classified a data sample to be an outlier based on the absence of a discriminatory peak or if the discriminatory peak is saturated. Low intensity or complete absence of a peak at a certain location can be caused due to limitations of the equipment to capture a particular wavelength. The nature of the plasma formed during the data collection process is the main cause of high intensity peaks. The data collection hardware can correctly record peaks in the spectra up to a certain maximum. If the intensity of the peaks is greater than this maximum, the equipment will clip the spectra leading to saturated peaks. The samples are classified as explosive or non-explosive based on peak energies of

discriminatory peaks. Thus, such outliers, if not removed from the training data set, severely affect the discriminating model. The discriminatory peaks were first identified using partial least squares – discriminant analysis (PLS-DA), which is explained in detail in Sec 4.2. The samples which had the discriminatory peaks either absent or saturated were removed from the training data set. If left in the training data, these outliers would bias the discriminating model and severely affect the performance.

4.2 PARTIAL LEAST SQUARES – DISCRIMINANT ANALYSIS

Statistical techniques like Principal Component Analysis (PCA) are useful for capturing variance within a certain class. Image compression applications use PCA to transform a large set of correlated variables into a smaller set of uncorrelated variables. PCA fails to discriminate classes because it does not make an attempt to find directions in the sample data space. Partial Least Square – Discriminant Analysis (PLS-DA) addresses this issue directly. PLS-DA is a multivariate discrimination method specifically used to classify samples. It is essentially an inverse least squares approach to Linear Discriminant Analysis (LDA) and produces similar results but with noise reduction and variable selection which are characteristics of PLS.

In PLS-DA, the model that predicts the class number for each sample is developed using the Partial Least Squares (PLS) method. In the data set, there are two modeled classes: explosive and non-explosive. A variable with value closer to one indicates that it belongs to the explosive class whereas variables with value of zero indicate that it belongs to the non-explosive class. The PLS model does not predict either one or zero value exactly. Hence, a threshold is set, above which the variable is considered to be in the explosive class and below which the variable is deemed as non-explosive. By default, this threshold is set to 0.5. The training data set has known sample types, which help in estimating the threshold value. A PLS-DA model with a large number of latent variables can be used for discrimination between explosive and non-explosive sample types. A large number of latent variables ensures maximum amount of variance being captured but would make the PLS model rigid and any variation in testing

data would lead to inaccurate discrimination. Thus, PLS-DA by itself is not suitable for detection especially when peak shifts in spectral data are common. Instead, the weights of the latent variables where used to identify discriminatory peaks.

The PLS model was developed using PLS Toolbox 4.2 running under MATLAB. Three latent variables were used for creating the model. Three latent variables successfully captured around 90% - 95% of the variance, with the first two latent variables capturing 85% - 87% of the variance. Thus, the weights of the first two latent variables provided a good estimate about the regions in the spectra which could be used to discriminate the two classes. The peaks, in the regions indicated by the weights of the latent variables, were found to be better detectors of explosive sample type. The input data was first mean-centered and auto-scaled before generating the PLS model. During the mean-centering process, the mean of each column of the input matrix is calculated and subtracted from the respective column. After mean-centering the data includes only how that row differs from the average sample in the original data matrix. The auto-scaling process divides each column by the standard deviation of that column. The mean-centering and auto-scaling process ensures that each column of the input matrix has as mean of zero and a standard deviation of one. Figure 4.1 shows the weights of first two latent variables. The wavelength indices that had greater weights were considered to be symbolic of discriminatory peaks.

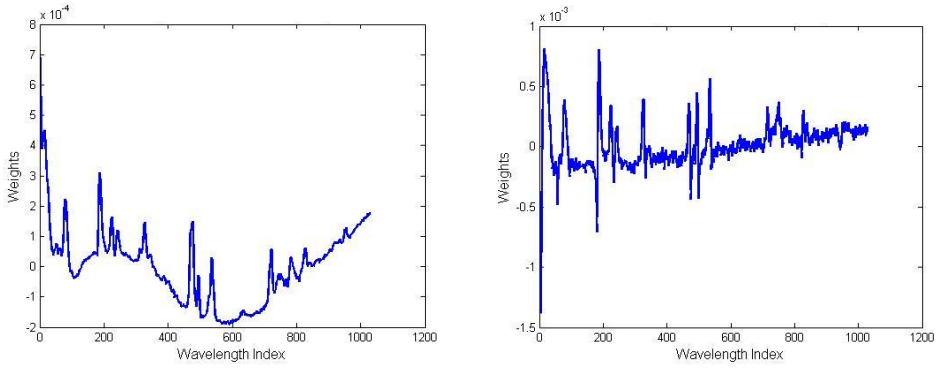

Figure 4.1. Weight vector of latent variables for specimen B explosive samples

5 SIGNAL PROCESSING PROCEDURES

5.1 SIGNAL DENOISING USING WAVELET TRANSFORM

The Raman spectra, obtained by using the experimental setup discussed in Section 3, contains noise along with the vital spectral information. The main sources of noise in Raman spectra are cosmic rays, shot noise and thermal noise. The statistics of the noise in the Raman spectra usually follows a Poisson process because of the random decay nature of the Raman process. Figure 5.1 shows an example of a noisy Raman spectrum. A denoising filter was implemented to remove the noise present in the spectra before performing further analysis. A wavelet based signal denoising algorithm was implemented to attenuate the noise in the signal. The signal denoising algorithm based on wavelet shrinkage is discussed in further detail in this section.

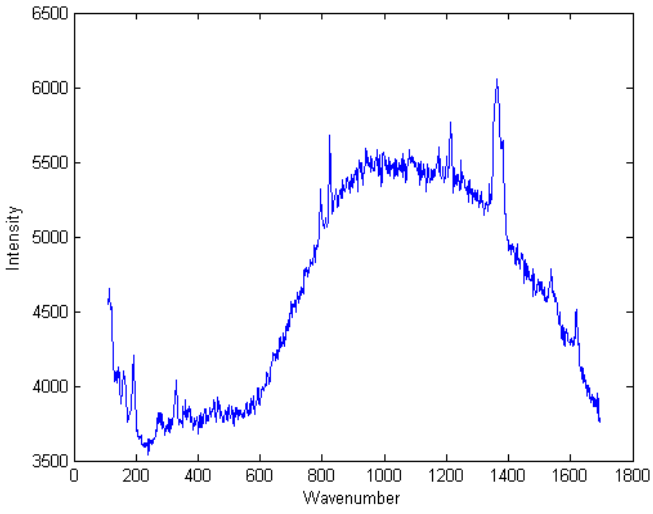

Figure 5.1. A noisy Raman spectra of specimen D explosive sample

5.1.1 Multi-Resolution Analysis. The wavelet transform based signal denoising approach attempts to remove the noise coefficients from the original signal by applying thresholding techniques. Signal denoising using wavelets is based on multi-resolution analysis [4]. The discrete wavelet transform (DWT) and the fast wavelet transform (FWT) are based on multi-resolution analysis. The multi-resolution analysis of the space $L^2(R)$ is discussed below, where $L^2(R)$ is the vector space of the one-dimensional function f(x). Z and R are the set of integer and real numbers respectively.

$L^2(R)$ consists of a sequence of nested subspaces:

where the basis of the subspace V_j is a set of orthonormal, translated functions, and each of these functions sets is a fixed dilation of the scaling function .

All the subspaces have the property:

V_{j-1} can be obtained in terms of W_j which is the orthogonal compliment of V_j .

The orthogonal basis of the subspace W_j is formed by the wavelet basis . For $j < n_0$;

and a signal x(n) can be decomposed by

Where,

: Discrete detail coefficients of the signal at level j

: Approximation coefficients of the signal at level j

$h(n)$ and $g(n)$: low pass and high pass filter respectively connected by

$g(n)=(-1)^{-n\ g(n)}\ h(N-n)$, where N : length of the filter

The signal reconstruction is based on

5.1.2 Signal Denoising Process. The implemented signal denoising algorithm using wavelet thresholding can be summarized as shown in Figure 5.2. The MATLAB function '*wavedec*' was used to decompose the input signal into *nL* levels. The '*wavedec*' function returns a decomposition structure which contains the wavelet decomposition vector *C* and a bookkeeping vector *L*. The signal was decomposed using the Daubechies wavelet family.

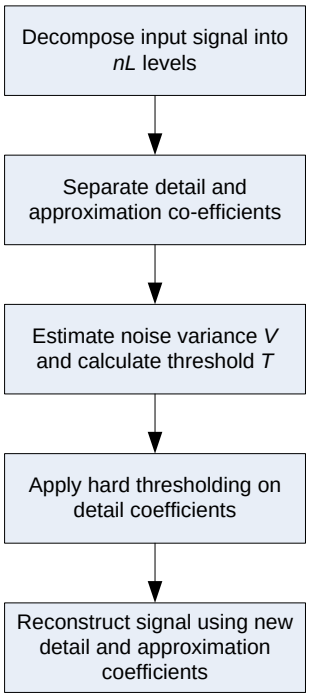

Figure 5.2. Signal denoising process

The decomposition vector *C* contains approximation and detail coefficients and has structure as shown in Figure 5.3 below.

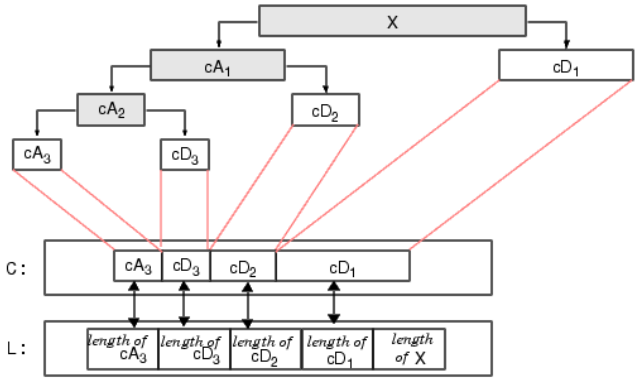

Figure 5.3. Structure of decomposition vector C and bookkeeping vector L

After separating the detail and approximation coefficients from the decomposition structure *C*, the variance of the noise is estimated using the detail coefficients. Donoho and Johnstone [5] explained the process of estimating noise using the detail coefficients. Donoho and Johnstone applied the wavelet thresholding method to eliminate the detail coefficients, which constitutes the noise in the signal. The optimal threshold is considered to be σ_w sqrt(2log(N)), where σ_w^2 is the noise variance and N is the data length. A hard thresholding technique was applied to the detail coefficients using the optimal threshold. Hard thresholding sets any coefficient less than or equal to the optimal threshold to zero. Hard thresholding was selected over soft thresholding because the sharp features of the signal are better represented in hard thresholding. Soft thresholding tends to smooth the signal which is not desirable. Soft thresholding shows better results when applied to natural images. After the detail coefficients have been thresholded, the signal is reconstructed using the '*waverec*' MATLAB function. Figure 5.4 below shows Raman spectra and denoised spectra of a single specimen E sample.

5.2 AUTOMATIC CURVE FITTING

Shah [3] describes the need for curve fitting in case of LIBS spectra. Automatic curve fitting is essentially an extension of the curve fitting procedure described in [3] applied to the Raman spectra. The automatic curve fitting algorithm is a recursive process used for calculating peak energies in the Raman spectra. This section describes the details of the automatic curve fitting process. For the Raman spectra, the location of peaks and their energy are the signature of a sample. Each peak in the spectra corresponds to an element which is unique in terms of strength and location for the sample type. The energy of the elemental peak corresponds to the concentration of the sample. Thus, energy of certain peaks or a combination of peaks (ratio) is often a good identifier of a sample type. Peak energies were considered instead of peak strengths because of the vulnerability of peak strengths to noise. Any change in DC level of the signal adversely affects the peak strengths. Using such vulnerable peak strengths as discriminators can lead to misclassification. Thus, peak energies need to be accurately calculated so that they can be used for discrimination of samples.

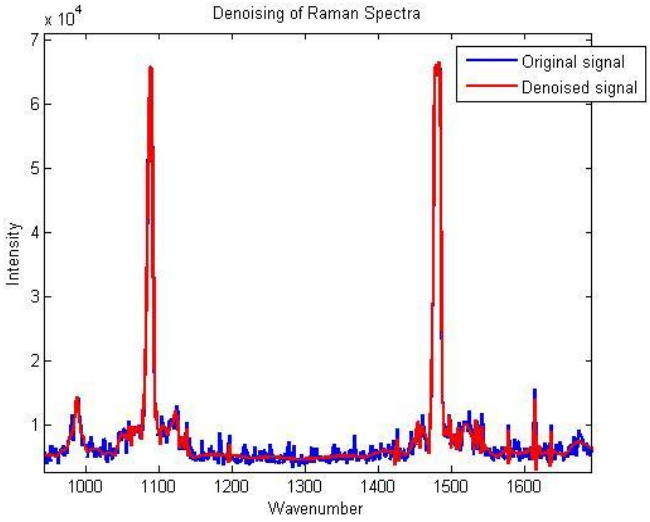

Figure 5.4. Denoising of a specimen E Raman spectra

It has been observed that Lorentzian or Gaussian distribution functions can accurately represent peaks in the spectra and hence these distributions are often used in spectroscopy to calculate energy of peaks. The Lorentzian and Gaussian distribution are described below:

As described in [3], the spectra of a sample can be expressed as a sum of Lorentzian and/or Gaussian peaks, the DC baseline and noise which are all functions of wavenumbers. Thus the model for the observed spectra, $s(x)$ can be represented as:

In manual fitting, initial values for pre-identified peak locations μ, and their corresponding peak widths γ values along with the locations where the dc baseline has to be estimated, have to be provided as input to the fitting algorithm. Considering the variations in peak locations and the constraint on range of wavelengths i.e. the selection of regions in manual fitting, peaks are often missed. Also, if a discriminatory peak is present close to another peak with significantly greater energy, it may not be fitted at all. Such peaks are called side-peaks. For these reasons, a fully automated and iterative fitting

algorithm was implemented. The input to this algorithm is the data to be fitted. The algorithm finds the locations of all existing peaks in a spectrum. The small peaks corresponding to noise are rejected by obtaining a signal-to-noise ratio for the spectrum. The algorithm also finds locations suitable for modeling of the dc baseline. Thus, the curve fitting process is fully automated with minimal user intervention. Figure 5.5 Results of automatic fitting process for specimen A sample where peak locations and DC baseline are automatically picked (a), shows the fitting result after the first iteration. The residual signal is calculated and second fitting iteration is performed. Figure 5.5 Results of automatic fitting process for specimen A sample where peak locations and DC baseline are automatically picked (c), shows the residual signal and Figure 5.5 Results of automatic fitting process for specimen A sample where peak locations and DC baseline are automatically picked (b), shows the fitting result after the second iteration. It can be observed from the figures that peaks that are missed during the first iteration are dealt with in the second iteration. Thus, the automatic curve fitting process generates a complete set of peak energies for all the peaks in the spectra.

Curve fitting is iteratively performed on the spectrum with these parameters. The first step is to fit the previously obtained peaks in the original spectrum as shown in Figure 5.5 Results of automatic fitting process for specimen A sample where peak locations and DC baseline are automatically picked (a). A signal comprising of these peaks is subtracted from the original spectrum and a residual signal is obtained and is shown in Figure 5.5 Results of automatic fitting process for specimen A sample where peak locations and DC baseline are automatically picked (c). The algorithm searches for any peaks in this residual signal and appends it to the list of peak locations obtained earlier. During this process, a new set of locations, which is an extension of the first set, for the removal of dc baseline is also obtained. Curve fitting is again performed on the original signal with the appended parameters. Figure 5.5 Results of automatic fitting process for specimen A sample where peak locations and DC baseline are automatically picked (b), shows the fitting result after the second iteration.

The peak locations obtained by the curve fitting are scanned for existence of the pre-identified discriminating peaks. A fitted peak location within a constraint is selected

as the peak location corresponding to the required peak and its peak energy (α) value is used for discriminatory purposes.

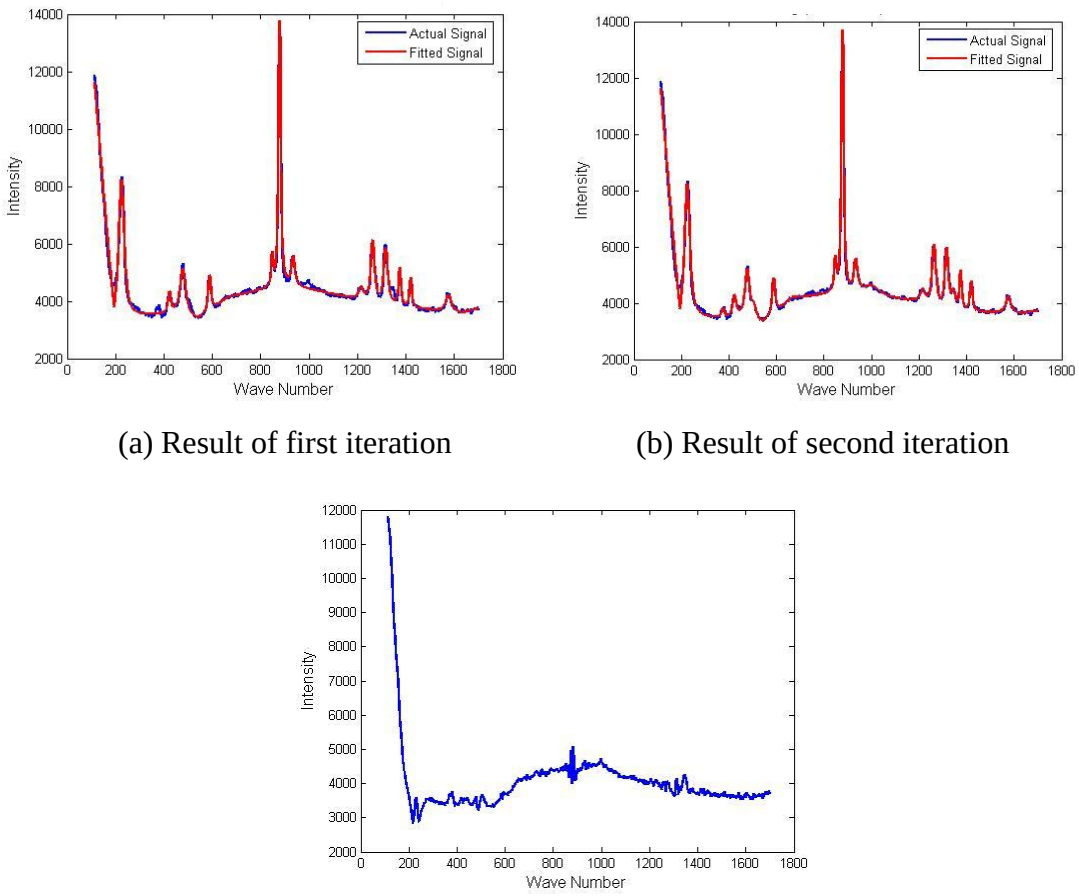

(a) Result of first iteration

(b) Result of second iteration

(c) Residual signal obtained after first iteration

Figure 5.5. Results of automatic fitting process for specimen A sample where peak locations and DC baseline are automatically picked

5.3 RAMAN DETECTORS

The Raman dataset consisted of several explosives. Each explosive sample type had different sets of discriminators which were selected based on the weights vector obtained from the PLS-DA process. For specimen E Raman spectra, the presence or absence of a discriminatory peak was sufficient for classification. A combination of peak energies (α) was used as discriminators for other explosive samples. A normalizer peak can be defined as a peak in the spectrum whose energy remains constant for all sample types. Thus, a normalizer peak will have constant energy for explosive and non-explosive sample type. The energy of a discriminatory peak was normalized by the energy of a normalizer peak in order to negate the effects of experiment and ambient conditions. A normalized α value of a discriminatory peak is denoted as feature value or peak energy ratios [3].

A combination of two or more feature values was used to form a linear discriminator. Although, adding more feature values to the linear discriminator increased the PD, it also increased the PFA which is undesirable. Thus, a maximum of three feature values were used to form the linear discriminator. Three linear discriminators for each type of explosive were selected with two or three feature values. Thus, each linear discriminator constitutes of two or more feature values. Table 5.1 shows the linear discriminator list for specimen A, B, C and D respectively. The terms (x + y + z) denotes the sum of energies of the peaks at locations x, y and z respectively. The feature values in Table 5.1 are ratios of peak strengths shown in a/b format and calculated as a/(a+b), in order to constraint the feature value between 0 and 1 [3].

The specimen E spectra used for multi-sensor fusion analysis did not require a linear discriminator. The strengths of certain peaks were directly considered as discriminators and a decision was based on them. These peak strengths were converted to decision values using [10],

Where, d: decision value

x: peak strength

σ: standard deviation of the spectra used as noise baseline

Table 5.1. Discriminator list and feature values for different explosive samples

Discriminator no.	Feature value 1	Feature value 2	Feature value 3
1	187/(1260+1320+1380)	475/(1260+1320+1380)	
2	475/(1260+1320+1380)	878/(1260+1320+1380)	
3	187/(1575)	475/(1575)	878/(1575)

(a) Discriminator list for specimen A explosive sample type

Discriminator no.	Feature value 1	Feature value 2	Feature value 3
1	232/(940)	840/(940)	
2	400/(1220)	840/(1220)	
3	232/(1220)	400/(1220)	840/(1220)

(b) Discriminator list for specimen B explosive sample type

Discriminator no.	Feature value 1	Feature value 2	Feature value 3
1	146/874	228/874	
2	146/874	1291/874	
3	228/874	622/874	1291/874

(c) Discriminator list for specimen C explosive sample type

Discriminator no.	Feature value 1	Feature value 2
1	192/1213	823/1213
2	192/1535	1360/1535
3	327/1213	823/1213

(d) Discriminator list for specimen D explosive sample type

Table 5.2 below shows the list of discriminatory features for Raman and LIBS for specimen E fusion data. For the specimen E spectra, five peak locations were used for discrimination, located at wavenumbers 1050 cm^{-1}, 1292 cm^{-1}, 1415 cm^{-1}, 1462 cm^{-1}

and1660 cm^{-1}. The maximum of their decision values was considered as the final decision corresponding to that sample.

Table 5.2. LIBS and Raman features for fusion on specimen E samples

LIBS features	**Raman features**
301/(333+344)	1050
	1292
248/(333+344)	1415
	1462
	1660

5.4 MULTI-SENSOR FUSION – DECISION LEVEL RAMAN AND LIBS FUSION

As mentioned in Section 3, spectra used for multi-sensor fusion of LIBS and Raman were obtained from specimen E. The LIBS spectra were processed as discussed by Shah [3] and Raman spectra were processed as described in the above sections. The fusion LIBS data consisted of only specimen E samples and the normal LIBS data consisted of specimen A and D samples. Therefore, the feature values used for discrimination of fusion LIBS data were different than the feature values used for discrimination of normal LIBS data. The features used for fusion LIBS spectra are 248/(333+344) and 301/(333+344). For Raman spectra, each feature was considered to be the peak value at locations 1050 cm^{-1}, 1292 cm^{-1}, 1415 cm^{-1}, 1462 cm^{-1} and1660 cm^{-1} respectively. Decision values for the Raman features were calculated using Equation 5.3. Decision values obtained from LIBS and Raman detection from the same region were fused using multi-sensor fusion.

The sample space consisted of five spots with specimen E explosive of varying concentration, with spot 1 having highest concentration and spot 5 having lowest concentration. The spots with low concentration i.e. Spot 4 and 5 were considered to be non-explosive whereas the spots with higher concentration i.e. spots 1, 2 and 3, were treated as explosives. All available spectra for LIBS and Raman fusion data would belong to either one of the spots. LIBS fusion data was analyzed separately using the feature values mentioned above and decisions for each of the five spots were generated. Similarly, Raman ammonium nitrate fusion data was analyzed and a decision value for each spot was obtained. The decision values from both LIBS and Raman were used to train a two dimensional linear discriminator which was used for classification of each sample.

6 RESULTS

6.1 RAMAN DETECTORS

As discussed in Section 5.3, several Raman detectors (discriminators) were used for identifying explosive sample types. The Raman data set analyzed consisted of five explosive specimen – A, B, C, D and E. The discriminators depend upon the type of explosive and hence each explosive sample type has a specific set of detectors. The discriminators for each explosive type were selected based on the PLS-DA weights vector, as discussed in Section 4.2. Table 6.1 below shows the performance of detectors for each explosive type. For a particular explosive type, the table consists of three discriminators used for analysis and a comparison between manual fitting process and automatic fitting process in terms of Probability of Detection (PD) and Probability of False Alarms (PFA). All entries in the table are in the form of $x \pm y$, where x is the base probability and y is the variance in the probability. A large value of y indicates higher uncertainty in the base probability x. In Table 6.1, the discriminators D1, D2 and D3 are equivalent to the discriminators in Table 5.1 for each explosive type. For each explosive type and discriminator combination, PD and PFA are calculated for automatic and manual fitting process. It can be observed that the results for automatic fitting process are equivalent or even better than the manual fitting process in some cases.

Figure 6.1 below shows the Receiver operating characteristic (ROC) curves for the four types of explosives – specimen A, B, C and D. The curves plot the Probability of Detection against the Probability of False Alarms and are symbolic of the performance of the algorithm for different explosive sample types. The figure shows the ROC curves for a single Discriminator type for each of the explosive sample types. In Figure 6.1, discriminator 1, discriminator 3, discriminator 3 and discriminator 2 were used for specimen A, B, C and D explosive types respectively. The list of discriminators for each sample type is shown in Table 5.1.

Table 6.1. Probability of Detection and Probability of False Alarms for different explosive types

Explosive Type	Fitting Type	Discriminators					
		D1		D2		D3	
		PD	PFA	PD	PFA	PD	PFA
A	Automatic	0.82 ± 0.18	0.42 ± 0.09	1 ± 0	0.40 ± 0.09	1 ± 0	0.46 ± 0.09
	Manual	1 ± 0	0.56 ±0.09	1 ± 0	0.46 ± 0.09	1 ± 0	0.48 ± 0.09
B	Automatic	0.90 ± 0.17	0.28 ± 0.09	1 ± 0	0.26 ± 0.09	0.90 ± 0.17	0.23 ± 0.09
	Manual	1 ± 0	0.40 ±0.09	1 ± 0	0.26 ± 0.09	1 ± 0	0.36 ± 0.09
C	Automatic	0.70 ± 0.21	0.32 ± 0.09	1 ± 0	0.34 ± 0.09	0.90 ± 0.17	0.38 ± 0.09
	Manual	0.60 ± 0.22	0.56 ±0.09	1 ± 0	0.30 ± 0.09	1 ± 0	0.30 ± 0.09
D	Automatic	0.86 ± 0.12	0.18 ± 0.08	0.73 ± 0.13	0.38 ± 0.09	0.86 ± 0.12	0.18 ± 0.08
	Manual	0.69 ± 0.14	0.32 ±0.09	0.95 ± 0.09	0.34 ± 0.09	0.69 ± 0.14	0.36 ± 0.09

6.2 MULTI-SENSOR FUSION

Raman and LIBS ammonium nitrate spectra from the same region were used as observations for fusion. For decision level fusion, decision values from LIBS and Raman classifiers were used to train a two dimensional linear discriminator as discussed earlier in Section 5.4. Fusion of LIBS and Raman spectra results in improved overall results

which are better than either of the two sensors individually. As seen in Fig. 6.2, there is a noticeable decrease in the false alarm rate and increase in detection rate using fusion for a given detection level. However, it is important to note that the LIBS detection is significantly poorer as compared to Raman in this case due to poor detection of AN with LIBS. Also the results reported here are based on very limited data.

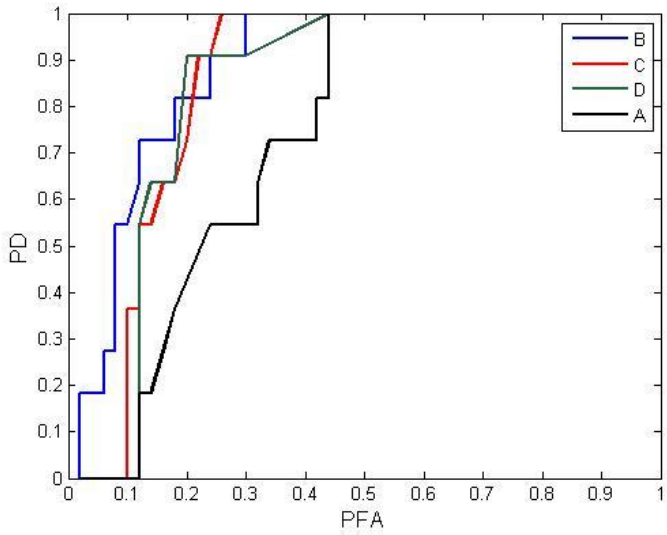

Figure 6.1. ROC curves for different explosive types

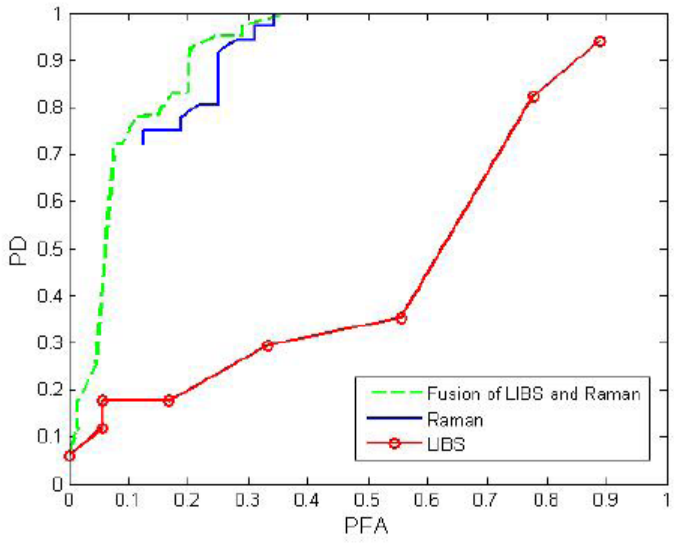

Figure 6.2. ROC curve showing results of decision level Raman and LIBS fusion

7 CONCLUSION

Raman spectra of various explosives types were analyzed with the goal to find the best discriminators for identification of different explosives samples in trace amounts at standoff distances. Signal pre-processing techniques were applied to remove outliers from the obtained Raman dataset and to find better discriminatory features in the spectra. Signal processing techniques like signal denoising, signal modeling, etc. were developed in order to compensate for the nature of the Raman spectra obtained. Furthermore, Raman and LIBS decision level multi-sensor fusion was developed and tested for the ammonium nitrate dataset. The specimen A detector successfully detected 100% of the samples with around 40% probability of false alarms. The specimen B detector produced 100% probability of detection with the probability of false alarms around 26%. The best specimen C detector could detect 100% of the samples with a false alarm rate of 34%. The specimen D detector detected 86% of the samples with a probability of false alarm around 18%. Decision level multi-sensor fusion results showed that the combination of Raman and LIBS tend to increase the probability of detection and reduce the probability of false alarms as compared to LIBS and Raman alone. It was observed that the performance of automatic curve fitting process was comparable or in some cases better than the performance of manual curve fitting process.

Thus, Raman spectroscopy proves to be effective in detection of trace explosives at standoff distances. The performance of standalone Raman is better for certain precursors like specimen E, whereas LIBS performs better in case of specimen A and D explosive samples. By combining Raman and LIBS, the performance of the overall system can be increased for detection of a wider variety of explosive samples.

APPENDIX

This section describes some of the important functions used while training and testing Raman data. Functions involved with Signal denoising and Automatic curve fitting process are explained.

[locsDC] = getBaseline(myWL, sig, res, minSTR);

This function is used to estimate the DC baseline of the given signal. It returns a vector *locsDC* which is used during the automatic curve fitting process. The *locsDC* vector will always contain the first and last values of *myWL* and some selected valley locations.

[pLocs, pidx, vLocs, vidx] = getPeakAndValleyLocs(myWL, mySig, minSTR, N)

This is an important function used by several other functions to get locations of all peaks and valleys in the selected spectra. One of the inputs to the function is the minimum strength of the signal (*minSTR),* which is calculated before calling the function. The minimum strength of the signal is calculated based on the standard deviation of the elements of the high pass signal, whose absolute value is less than a certain threshold.

Data = automaticFittingRaman(data)

This is the main function used for performing automatic curve fitting. The input to this function is the structure *data* which has the signal on which curve fitting has to be performed. The function automatically selects the peaks to be fit and estimates the DC baseline. It performs recursive curve fitting where residue is calculated once a signal is fitted and fitting is again performed on the signal based on the peaks in the residual signal. The number of times curve fitting is to be performed can be changed through the code. After maximum number of times curve fitting is performed, the fitting results are added into the *data* structure. A new field *spectra* holds the fitting results.

[alphasAll] = getAlphas (TrainData,peakSelectType,ExpType)

This function takes as input the fitted data *TrainData,* automatic or manual peak select type *peakSelectType* and explosive type *ExpType*. Based on the inputs this

functions generates a matrix *alphasAll* which contains the peak energies (α) of all the fitted peaks for a particular explosive type and peak select type. This function sums up the alpha values of peak within a range and compensates for shifting peaks.

[vals,idToUse,features]= getRamanFeatures(alphasAll,peakSelectType,ExpType)

This function returns the description of the discriminatory features depending upon the inputs *peakSelectType* and *ExpType.*

[vals, idToUse] = getFeatureVals(sigs, feats)

The input to this function is *sigs* which is the *alphasall* matrix for automatic fitting process or sum of peak energies calculated in the *getRamanFeatures* function for the manual fitting process. The other input to this function is *feats* that contain the column numbers of the summed peak energies which are considered for a particular feature value. It returns the feature values *vals* and *idToUse* containing the data ids used for training.

[func, AllCoeff] = trainThresh(myVals, discrim, myY, fitType)

The inputs to this function include *myVals* which is returned by *getRamanFeatures* function, *discrim* contains the column numbers from *myVals* that should be combined in order to obtain the discriminator, *myY* contains the classification of the sample i.e. either 0 or 1, *fitType* describes the discriminator to be used i.e. linear, quadratic or mahalanobis. This function is used to generate the discriminator.

[sigD] = getDenoisedSig_v2(sig,varargin)

This function takes as input the original signal and returns the denoised signal. It can take a variable input which can be type of wavelet used for denoising the signal. By default, ‘sym8’ wavelet type is used. This function used ‘wavedec’ and ‘waverec’ MATLAB functions.

BIBLOGRAPHY

[1] *Existing and Potential Standoff Explosives Detection Techniques*, National Academies Press, 2004.

[2] R. D. Waterbury, E. L. Dottery, A. Ford, and J. Rose, "Results of a UV TEPS/Raman system for standoff detection of energetic materials," 26th Army Science Conference, 2008.

[3] P. Shah (2009), "MAXIMUM LIKELIHOOD FUSION FOR DETECTION OF IED PRECURSORS USING LASER-INDUCED BREAKDOWN SPECTROSCOPY," Unpublished dissertation. Missouri University of Science and Technology

[4] S. Mallat (1989), "A Theory for Multiresolution Signal Decomposition. The Wavelet Representation," IEEE Transactions on Pattern Analysis and Machine Intelligence 11 pp. 674-693

[5] D. Donoho and I. M. Johnstone, "Ideal spatial adaptation by wavelet shrinkage," Biometrika, pp. 425–455, 1994.

[6] Y.Yang, T.Li and Y.Li, "Explosives Detection Using Dual Energy X-ray Imaging and Photoneutron Analysis," 2009 IEEE Nuclear Science Symposium Conference Record, pp. 876-878

[7] R. Furstenberg, C. Kendziora, M. Papantonakis, S. Stepnowski, "Stand-off Detection of Trace Explosives by Infrared Photo-thermal Spectroscopy," Technologies for Homeland Security, 2009. HST '09. IEEE Conference, pp. 465-471

[8] S. Kong and D. Wu, "Terahertz Time-Domain Spectroscopy for Explosive Trace Detection," CIHSPS 2006 - IEEE International Conference on Computational Intelligence for Homeland Security and Personal Safety Alexandria, VA, USA, 16-17 October 2006

[9] T. Griffy, "A Model of Explosive Vapor Concentration II, In Advances in Analysis and Detection of Explosives," Proceedings of the 4th International Symposium on Analysis and Detection of Explosives, September 7-10, 1992, Jerusalem, Israel; J. Yinon, Ed; Kluwer Academic Publishers: Dordrecht, Netherlands, pp 503-511.

[10] P. Shah, A. Singh, S. Agarwal, and S. Sedigh, " Sensor data fusion for spectroscopy-based detection of explosives," 2009 Detection and Sensing of Mines, Explosive Objects, and obscured Targets XIV, Orlando, FL, USA

[11] F. DeLucia, A. Samuels, R. Harmon, R. Walters, K. McNesby, A. Lapointe, R. Winkel, and A. Miziolek, "Laser-induced breakdown spectroscopy (libs): A promising versatile chemical sensor technology for hazardous material detection," IEEE SENSORS JOURNAL 5, 681-689 (August 2005)

[12] J. Gottfried, F. DeLucia, C. Munson, C. Ford, and A. Miziolek, "Detection of energetic materials and explosive residues with laser-induced breakdown spectroscopy: Ii. Stand-off measurements," Final ARL-TR-4241, U.S. Army Research Laboratory, Aberdeen Proving Ground, MD 21005-50666 (September 2007)

[13] D. Alexander, D. Poulain, M. Ahmad, R. Kubik, E. Cespedes, "Environmental monitoring of soil contaminated with heavy metals using laser-induced breakdown spectroscopy," Geoscience and Remote Sensing Symposium, 1994. IGARSS '94. Surface and Atmospheric Remote Sensing: Technologies, Data Analysis and Interpretation, International, 767 - 769 vol.2 , 8-12 Aug. 1994

[14] R. Wentworth, J. Neiss, M. Nelson, P. Treado, "Standoff Raman hyperspectral imaging detection of explosives," Antennas and Propagation Society International Symposium, 2007 IEEE , vol., no., pp.4925-4928, 9-15 June 2007

[15] A. W. Miziolek, F. C. DeLucia Jr, C. Munson, J. L. Gottfried, R. Russo, P. J. Treado, and M. P. Nelson, "A new standoff CB detection technology based on the fusion of LIBS and Raman," http://www.chemimage.com/docs/publications/Threat-Detection/CBD Summary Final Rev.pdf, February 2009.

VITA

Abhijeet Singh, son of Dr. Rajanikant Singh and Meena Singh was born on December 30, 1985 in Mumbai, India. He received his Bachelor's of Engineering Degree in Electronics and Telecommunications from Thakur College of Engineering and Technology, University of Mumbai, India in June 2007. Abhijeet then began pursuing his Master's Degree in Electrical Engineering at Missouri University of Science and Technology, Rolla, USA under the guidance of Dr. Sanjeev Agarwal, Professor of Electrical and Computer Engineering Department.

During his graduate degree, Abhijeet worked as a Graduate Research Assistant with Airborne Reconnaissance and Image Analysis (ARIA) Lab at Missouri S&T. Abhijeet got his Master's in Electrical Engineering in December 2010.